Pulse-echo Ultrasonic NDE of Adhesive Bonds in Automotive Assembly

Roman Gr. MAEV, Sergey TITOV, University of Windsor, Windsor, Canada

Abstract. Recently, adhesive bonding technology has begun to play a more prominent role in automotive industry. Nondestructive evaluation of the adhesive joints is a challenging task for many reasons: access to the bond is only available from one side, the acoustic impedance mismatch between steel and the adhesive material is very large, and the thickness of the adhesive layer may be significantly varied. Many ultrasonic techniques for NDE of adhesive bonds have been proposed, including time and spectral domain methods. Generally speaking, however, the lateral resolution of these techniques is not high enough to facilitate the proper evaluation of automotive joints whose widths are typically 10 – 15 mm. To increase this resolution in the pulse–echo mode, we employed flat, highly damped ultrasonic transducers having an element size of approximately 3 - 6 mm. In this case, the small transducer diameter causes strong diffraction in the ultrasonic wave as well as mode conversion at the interfaces between the layers of the joint, resulting in a very complex received waveform. To detect disbonds within the joint, the echo signal is compared with a reference waveform that was obtained from the first metal sheet outside of the joint. In the case of disbonding at the front metal-adhesive interface, the received and reference waveforms are very close. Disbonds at the rear adhesive-metal interface cause a phase inversion of the reflected response; this can be estimated by reference waveform subtraction. The proposed technique has been tested using a set of steel and aluminum samples with the varying adhesive layer thicknesses.

Introduction

In recent years, adhesive bonding has become an integral part of automotive production technology. As such, the durability of adhesive joints is an essential element contributing to the overall strength and safety of the automobile. For this reason, it is necessary that quality assessment be incorporated directly within the production process. The numerous advantages of ultrasonic non-destructive evaluation methods make it perfectly suited for this application.

The body of a typical car is comprised of punched metal sheets with many joints consisting of two or more of these sheets (0.7–2 mm thickness) with layers of adhesive material between them. Thickness of the adhesive can vary between 0.1 and1 mm. Ultrasonic testing of these adhesive joints is difficult for two primary reasons: (1) the high acoustic impedance mismatch between the layers, and (2) the high attenuation of ultrasound inside the adhesive layer itself. Most research in this area is focused on the detection of void–disbonds at both the first metal/adhesive interface (closest to the transducer) and the second adhesive/metal interface (furthest from the transducer). Due to the great impedance mismatch between the adhesive and the metal (especially steel) there are strong, long lasting reverberations in the first sheet that effectively mask the small echoes that result from the second interface.

Many ultrasonic techniques have been proposed for NDT of the automotive adhesive joints [1]. Methods based on the decay rate of reverberations in the first sheet and measurement of the reflection coefficient [2], unfortunately, can only be used for the detection of disbonds at the first interface. To assess the integrity of the adhesive joint as a whole, a technique has been proposed in which the first through thickness low–frequency resonance of the joint is measured [3]. Despite the narrowing of the ultrasound beam by a specially designed collimator, low frequency resonance necessarily implies a restriction in the lateral resolution of these techniques—an attribute that is highly desirable in the evaluation of typical automotive joints. A higher degree of resolution could be potentially obtained using common pulse–echo technique. To reduce the amplitude of the reverberations in the first sheet and, in turn, to detect the phase of the echo from the second interface, digital signal processing algorithms based on inverse filtration have been developed [4–6]. However, the inverse procedure requires the exact waveform similarity of successive echoes. However, the inverse procedure requires the waveform to simultaneously resemble that of successive echoes. This requirement is not satisfied in cases of strong acoustic beam divergence and mode conversion at the interfaces between the layers. To extract the echoes from the second interface and estimate the reflection coefficient at the first interface, we propose a processing algorithm based on comparison of the output waveform with a previously recorded reference response from the first metal sheet outside of the joint.

1. Simplified wave model

In this paper, we consider the pulse–echo NDT of adhesive joints with flat interfaces and unknown adhesive layer thicknesses where only single side access is permitted. The classification of typical defects is presented in Fig. 1. In short, the method should distinguish three main cases: good joints (case C), void–disbonds at the first metal/adhesive interface or an altogether absence of adhesive material (case A), and void–disbonds at the second metal/adhesive interface or absence of the contact between the adhesive material and the second metal sheet (case B).

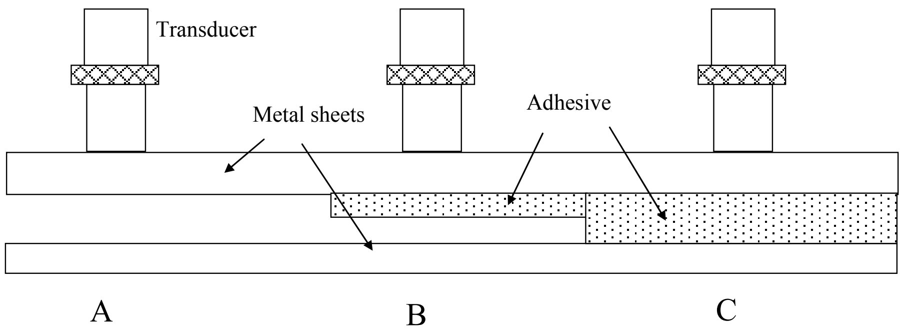

Figure 1. Types of defects: A – disbond at the first interface,
B – disbond at the second interface, C – good joint.

Amplitude calculations for multiple echoes received from multilayer structures have already been published (see, for example, [7]). Even in the case of a two-layer structure, the echo pattern can be rather complicated. In this study, the most pronounced set of pulses was selected. One set of pulses, a_n, is produced as the wave reverberates in the first metal sheet, where n is a number of the pulse, n=1, 2… Another set, b_n, is generated as the wave experiences a one-fold propagation within the adhesive layer, and is reflected from the second interface. There are also sets of pulses resulting from several reflections within the adhesive material. Due to strong attenuation, however, their amplitudes are considerably diminished. In addition, although there are numerous pulses generated from the propagation of the wave in the second metal sheet, due to low transmission, the amplitudes of the partial pulses are even smaller. As a result, they usually produce a noise–like output waveform.

Letting A_0 be the amplitude of the main bang pulse, the amplitudes of the reverberations in the first layer are:

$$a_n = -A_0 \cdot \left(\frac{T_0}{R_0} \right)^2 \cdot \left(R_0 \cdot |R_1| \cdot \eta_1 \right)^n = K \cdot \gamma_1^n \tag{1}$$

$$K = -A_0 \cdot \left(\frac{T_0}{R_0} \right)^2, \qquad \gamma_1 = R_0 \cdot |R_1| \cdot \eta_1 \tag{2}$$

where T_0, R_0 represent the transmission and reflection coefficients at the transducer/first sheet interface, and η_1 is the attenuation coefficient in the first sheet. The reflection coefficient at the first metal/adhesive interface R_1 is negative; moreover, in the case of disbond at the first interface $R_1 = -1$. The corresponding time delays of these pulses with respect to the main bang pulse are $n\tau_1$.

Let h_n be the amplitude of a pulse passed one time in the adhesive layer and $n-1$ times in the metal layer:

$$h_n = -a_n \cdot \left(\frac{T_1}{R_1} \right)^2 \cdot \left(R_1 \cdot R_2 \cdot \eta_2 \right) = -K \cdot \left(\frac{T_1}{R_1} \right)^2 \cdot \gamma_1^n \cdot \gamma_2 \tag{3}$$

$$\gamma_2 = |R_1| \cdot R_2 \cdot \eta_2 \tag{4}$$

T_1 and R_2 represent the transmission coefficient at the first interface and reflection coefficient at the second interface, respectively, and η_2 is the attenuation coefficient in the adhesive layer. For a good joint $R_2 > 0$, whereas, in the case of disbond at the second adhesive/metal interface $R_2 = -1$.

The time delays of these partial pulses are $n\tau_1 + \tau_2$. Thus, n partial pulses with amplitude h_n have the same time delay, and due to constructive interference, the resulting amplitude b_n is:

$$b_n = h_n \cdot n = -K \cdot \left(\frac{T_1}{R_1} \right)^2 \cdot \gamma_1^n \cdot \gamma_2 \cdot n \tag{5}$$

The amplitudes a_n, and b_n, calculated for the steel–epoxy adhesive joint, are presented in Fig. 2. The acoustical properties of the materials are listed in Table 1 where the attenuation coefficients used in the calculations were $\eta_1 = 1$, and $\eta_2 = 0.7$.

The output waveform can be represented as a superposition of several responses associated with the reflections at different interfaces of the joint. In case of a single metal sheet, the output waveform $s_0(t)$ consists of reverberating pulses having amplitudes a_{n0} (solid line in the left graph, Fig. 2). If the metal sheet is in contact with the adhesive, the response $s_1(t)$ produced by reflection at the first metal/adhesive interface has amplitudes a_n (dashed line).

Reflection at the second interface gives the response $s_2(t)$ which consists of the pulses with amplitudes b_n (doted line).

Table 1. Material properties.

Material	Density, kg/m^3	Velocity, m/s	Impedance, 10^6 kg m^{-2} s^{-1}
Polystyrene (transducer)	2340	1056	2.47
Steel, 1020	5890	7710	45.41
Aluminum	6320	2700	17.06
Adhesive (epoxy–based)	1150	2300	2.65

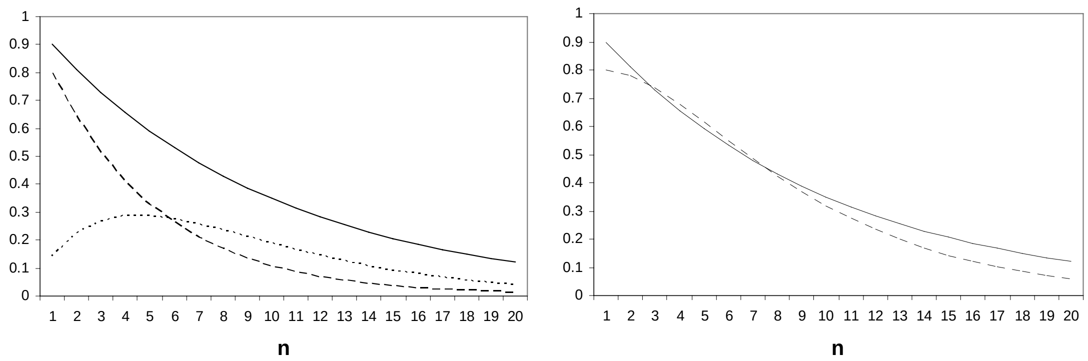

Figure 2. Calculated amplitudes of the responses: left graph – a_n, a_{n0} (solid and dashed lines), b_n (doted line); right graph – a_n (solid line), and $a_n + b_n$ (doted line).

The output waveform can be estimated as a sum of the responses $s(t)= s_1(t) + s_2(t)$ and numerous small pulses produced by multiple reflections inside the adhesive layer and the second metal sheet. The polarity of the response $s_2(t)$ depends on the impedance ratio at the second interface and can be used to detect disbond between the adhesive layer and the second metal sheet.

2. Signal processing

2.1 The first metal/adhesive interface

To evaluate the first interface, usually the difference between the decay rates of amplitudes is used [2]. This difference is quite notable for the responses $s_0(t)$, and $s_1(t)$, where $s_1(t)$ is a response obtained for a semi-infinite adhesive. In practice however, this discrimination should be undertaken between $s_0(t)$ and $s(t)= s_1(t) + s_2(t)$. The behavior of the amplitudes of the pulses $s(t)$ depends with time delay τ_2, and due to constructive interference, it may be very close to the decay of $s_0(t)$ as it is shown in the right graph of Fig. 2.

To detect disbond at the first interface, we propose to compare the waveform W (measured at the point of interest) with the reference waveform S_{ref} that was previously recorded outside of the joint. The estimated deviation of the difference $R=W–S_{ref}$ can be used as a measure of signal similarity, as it is shown in Fig. 3.

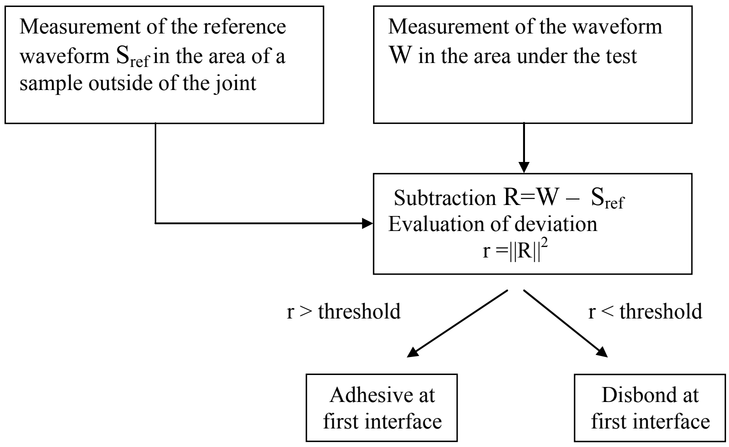

Figure 3. Signal processing algorithm for disband detection at the first interface.

2.2 The second adhesive/metal interface

To detect disbonds at the rear adhesive/second metal sheet interface, we propose to compare the measured waveform W with the reference waveform $S`_{ref}$, which simulates the reverberations in the first metal sheet in the case of a semi–infinite adhesive layer (Fig. 4). The waveform $S`_{ref}$ can be calculated based on the experimental waveform S_{ref} by introducing an additional damping. Therefore, the difference $W - S`_{ref}$ is an estimation of the response $s_2(t)$, where determining the phase allows a conclusion to be generated regarding disbond at the second interface.

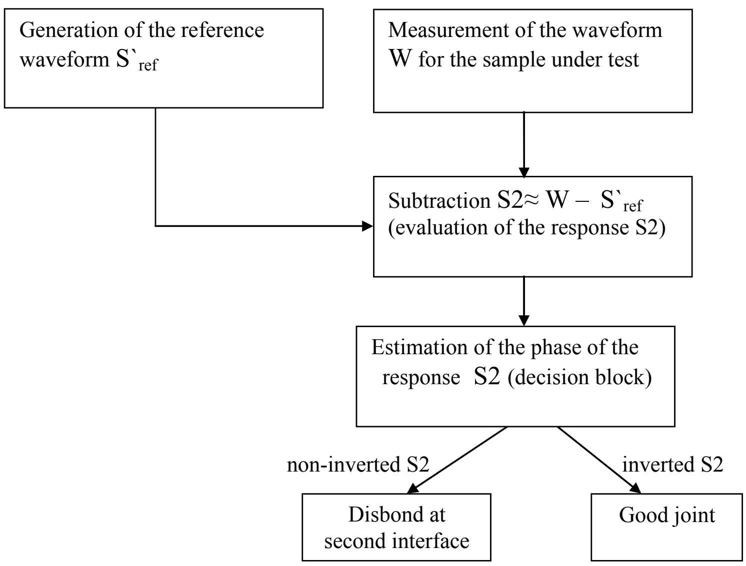

Figure 4. Signal processing algorithm for disband detection at the second interface

3. Experiment

3.1 Experimental setup

To confirm the proposed method, sets of steel and aluminium samples of types A, B, C (Fig. 1) were prepared. The thicknesses of the metal sheets were in the range of 0.7 – 2.0 mm, and the thickness of the adhesive layer gradually varied along the specimens from 0.1 up to 1 mm. A Panametrics V2099 removable delay line transducer having a 15 MHz central frequency and a 4 mm element size was used in the experiments.

3.2 The first adhesive/metal interface

To detect disbond at the first interface, the waveform *W* was compared with the reference waveform S_{ref}. The waveforms measured for the A, B, and C samples are shown in Figs. 5 and 6 as dashed lines. The deviation of $R=W–S_{ref}$ is very small for the single sheet, whereas the presence of the adhesive causes its notable increase.

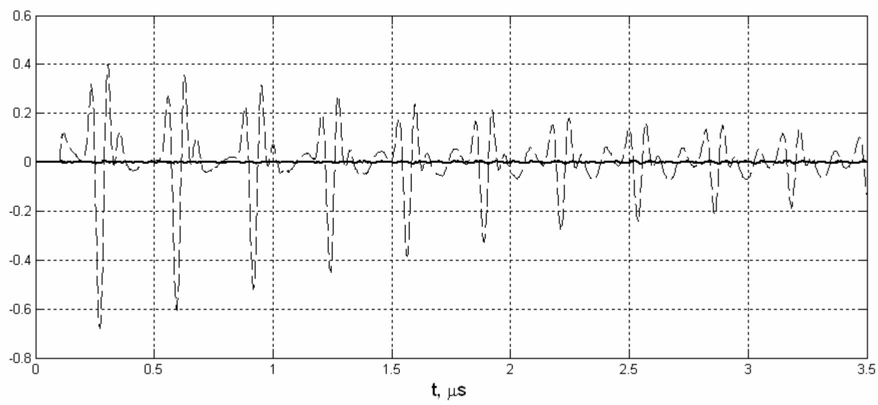

Figure 5. Waveform *W* (dashed line), $W–R_{ref}$ (solid line), obtained for 1mm steel sheet.

3.3 The second adhesive/metal interface

Fig. 7 shows the results of the signal processing following the algorithm presented in Fig. 4. Substation of the reference $S`_{ref}$ from the waveform *W* effectively suppresses the reverberations in the first metal sheet $s_1(t)$ and reveals residual responses. Among these responses, $s_2(t)$ is dominant. The amplitudes of $s_2(t)$ reach maximal values at $n=4$, which is in agreement with the theoretical model (Fig. 2). The time delay τ_2 between the pulses of the responses $s_2(t)$ and $s_1(t)$ is proportional to the thickness of the adhesive layer. The phase of $s_2(t)$ is non–inverted for the disbonded second interface, whereas a good contact at this interface causes the phase inversion.

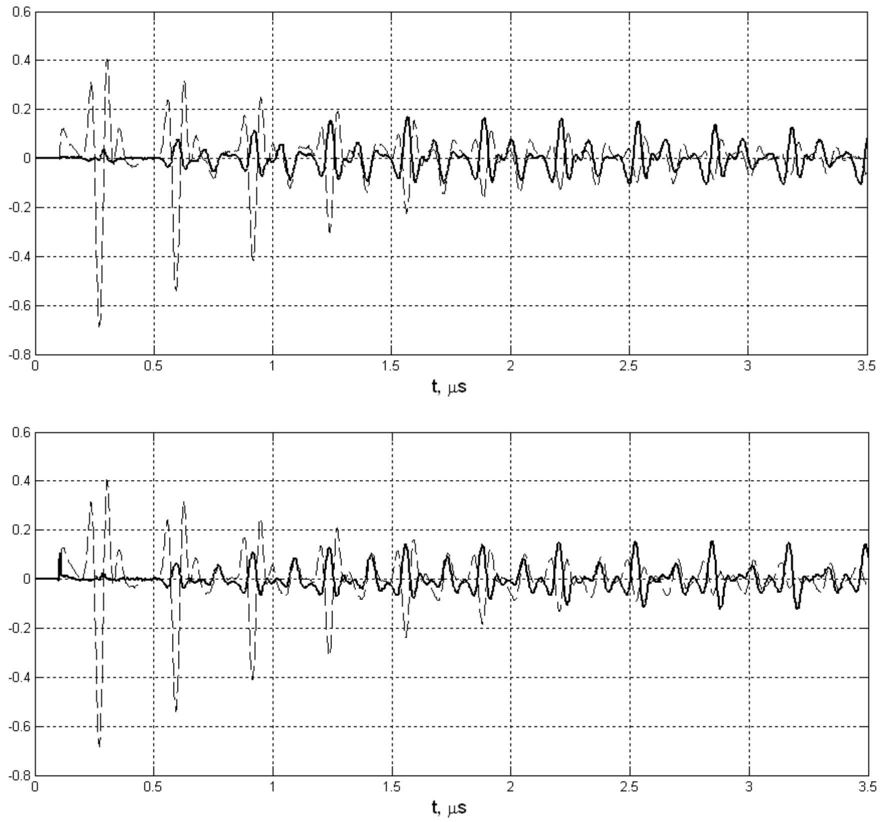

Figure 6. Waveform W (dashed line), $W\text{–}R_{ref}$ (solid line), obtained for a sample with disbond at the first interface (upper graph), and fully bonded (lower graph). The thickness of the adhesive is 0.6 mm.

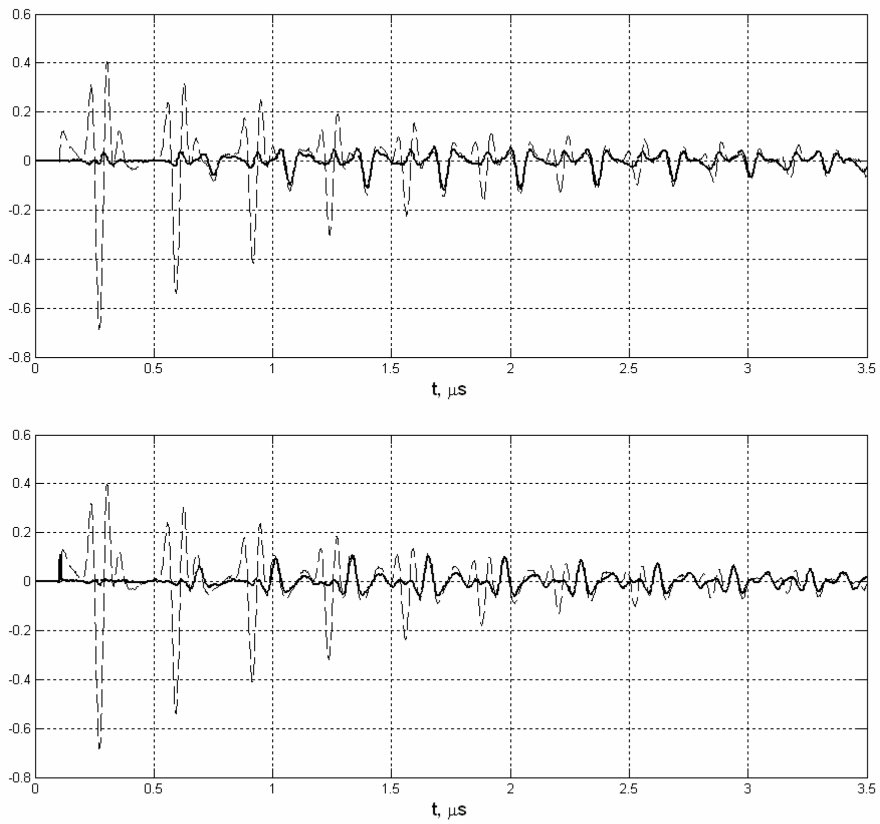

Figure 7. Waveform W (dashed line), $W\text{–}R`_{ref}$ (solid line), obtained for a sample with disbond at the second interface (upper graph), and fully bonded (lower graph). The thicknesses of the adhesive are 0.6 and 0.5 mm.

4. Conclusion

The proposed NDT method of the adhesive joints has been successfully tested for all combinations of steel (0.7, 1.0, 1.5, and 2.0 mm) and aluminium (1.1, and 2.5 mm) adherend, and for all thicknesses of the adhesive layer within the range of 0.1 – 1.0 mm.

References

[1] Adams R.D., Drinkwater B.W. Nondestructive testing of adhesively–bonded joints. NDT E Int., 1997, v. 30 (2), p. 93–98.

[2] Goglio L., Rosetto M. Ultrasonic testing of adhesive bonds of thin metal sheets. NDT E Int., 1999; v. 32 (6), p. 323–331.

[3] Robinson A.M., Drinkwater B.W., Allin J. Dry–coupled low–frequency ultrasonic wheel probes: application to adhesive bond inspection. NDT E Int., 2003 v. 36 (1), p. 27–36.

[4] Freemantle R.J., Charllis R.E., and White J.D.H. A Z–transform technique for thin–layer reverberation cancellation applied to ultrasonic NDT of adhered structures. IEE colloquium. Digest No. 1994/102. 7/1–7/4, 1994.

[5] Charllis R.E., Freemantle R.J., White J.D.H., and Wilkinson G.P. Ultrasonic compression wave NDT of adhered metal lap joints of uncertain dimensions. Insight, 1995, v. 37 (12), p. 954–963.

[6] Charllis R.E., Freemantle R.J., Wilkinson G.P., and White J.D.H. Compression wave NDE of adhered metal lap joints: uncertainties and echo feature extraction. Ultrasonics 1996, v. 34, p. 315–319.

[7] Krautkramer J., and Krautkramer H. Ultrasonic Testing of Materials. Springer-Verlag, N.Y., 1969, p. 253–255.